CHAPTER 4 GEOPHYSICAL SURVEY

Controlled Source Audio Frequency Magneto-Telluric (CSAMT) method, Spectral IP (SIP) method and IP method were conducted in Morro do Acampamento area over three years.

The CSAMT method was conducted in Phase I for the purpose of targeting promissing areas of mineralization using resistivity of structural analysis.

The SIP method was conducted for three years. The purpose of the method was to first pursue the C-1 ore body toward the lateral and vertical directions and to analyse the spectra characteristics returned from the C-1 ore body so that the characteristics can be employed in surveys in other areas.

Secondarily, the purpose was to analyse the detailed geological structure of the area and to detect the potential parts using spectral characteristics from the promissing areas extracted same method plus geochemical surveys.

The IP method was conducted to compensate for the space between SIP survey lines at the same time with SIP survey in Phase III.

Survey area is shown in Fig. III–6.

4–1 CSAMT Method

4–1–1 Contents of the Survey

CSAMT method is a electromagnetic technique Apparent resistivities are gained by measuring electric and magnetic fields when electric currents are sent with frequencies spanning 4 to 2048Hz.

Electric fields were measured by potential electrodes parallel to the current electrodes, which were set sufficiently apart from the measuring points so that the electromagnetic wave transmitted could be detected as plane waves. Magnetic fields were measured by sensore, which were set perpendicular to the current electrodes.

As the area covered by a pair of current electrodes is limited, four pairs were set out to cover the entire survey area. Two were set in the southern-most part of the area with the direction of E-W, and the other two were set farther south at a distance of 3 km from the former pairs in the same direction.

The distribution of resistivities on cross sections were structuraly analysed by computer. Resistivity structures were assumed in this area as shown in Fig. III–3, III–4 and III–5.

Table III - 4 Amounts of CSAMT Survey

Area Covered	Station Spacing	Current Electrode Separating	Number of Stations	
100 km² (10km × 10km)	400 m ~ 500 m	TX−1 2,000 m	56 pts.	202 pts.
		TX−2 2,000 m	42 pts.	
		TX−3 1,750 m	65 pts.	
		TX−4 2,000 m	39 pts.	

4–1–2 Results of the Survey

As for the distribution of resistivities, sudden changes are observed in some parts which are thought to be affected by structural lines or different neighbouring beds (Fig. III–6).

High, intermediate and low resistivity areas are divided by the discontinuous lines of resistivity values, which trend north and northeast.

High resistivity values ($\geqq$ 1000Ω·m) were mainly gained in the west, intermediate values (150Ω·m∿600Ω·m) were gained in the center and low values (< 100Ω·m) were gained in the east. The shape of the distribution is nearly the same from the shallowest to the deepest zones.

The high resistivity zone continues from the surface to the deeper part without changes of the value to the west of the survey area. In the high resistivity area schists and amphibolites are though to occur in very thick sequences because the lower frequencies are shifted higher the resistivities go up.

Intermediete and low resistivity areas are distributed in the central to eastern parts of the survey area. The Largest area makes a narrow zone trending to the north in the central part just like dividing the area into two parts.

That area is possibly due to the presence of a fracture zone. The areas in the east correspond to amphibolite in the shallower parts.

As a result of structural analysis performed on resistivity, low resistivity distributions with thickness of 100m from the surface and high resistivity with more than 1000Ω·m distributions belo a depth of 100m. High resistivity zones corresport to amphibolite and acidic schists or the basement.

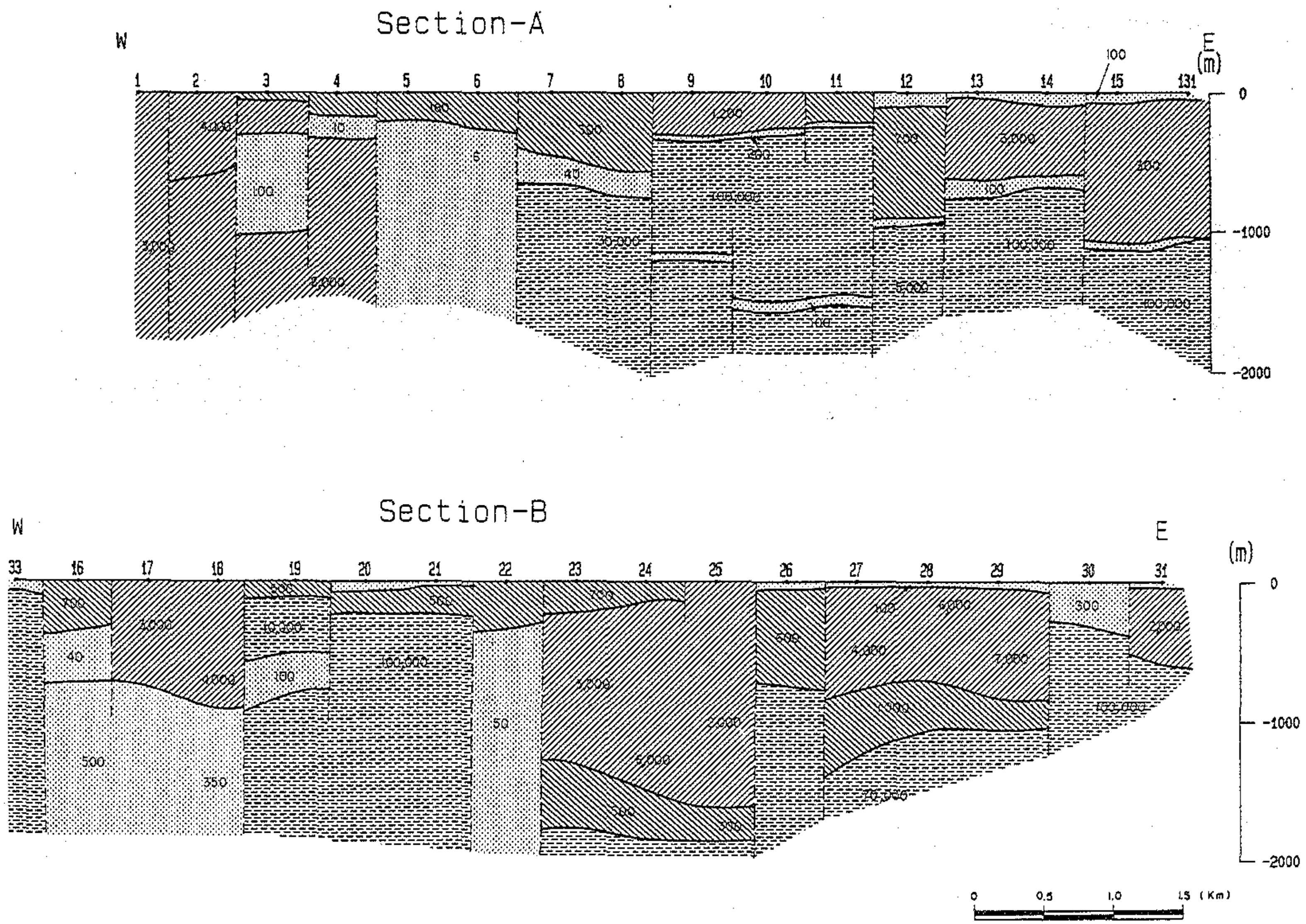

Fig. III - 3 CSAMT Interpreted Resistivity Sections (Section A and B in Fig. III-6)

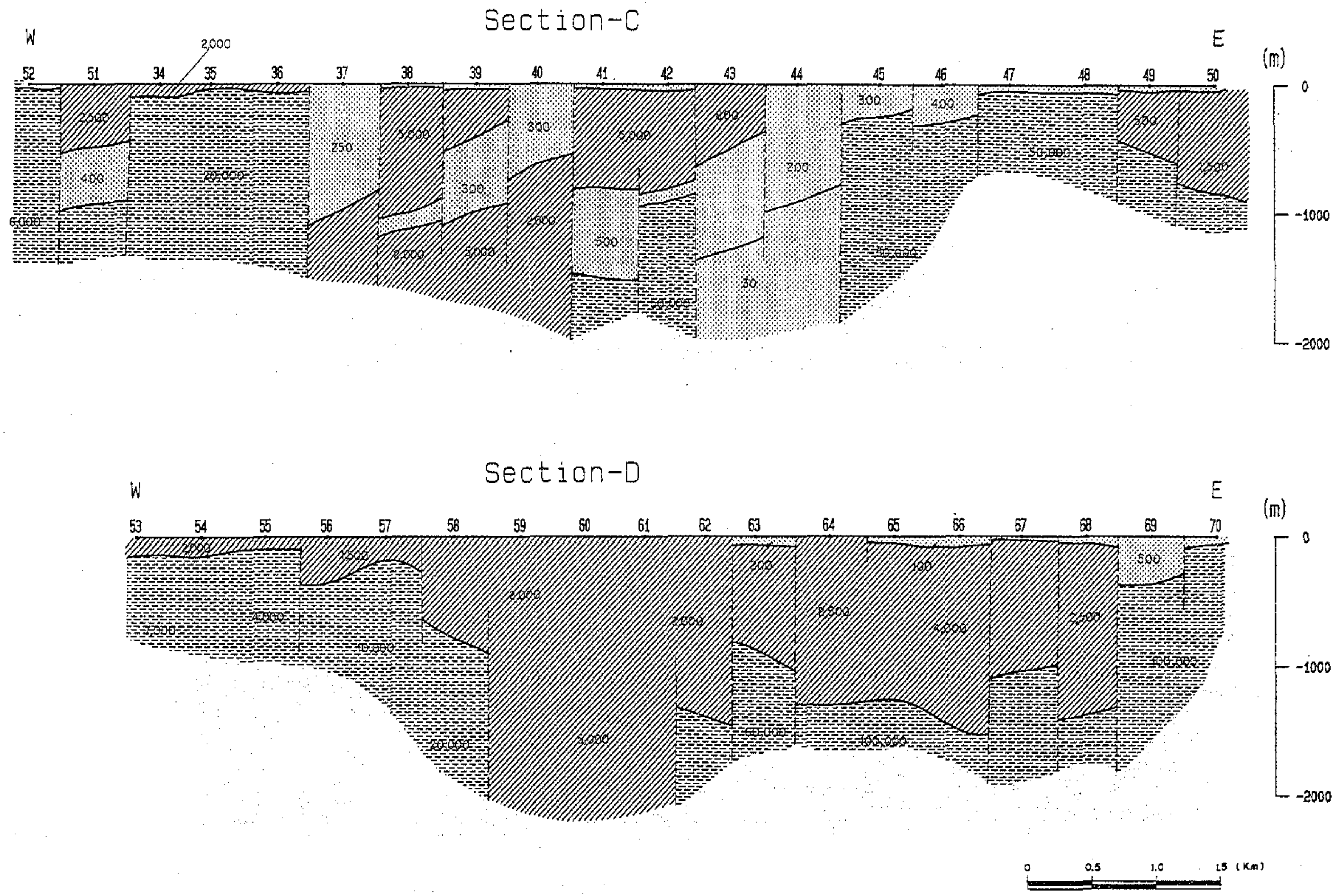

Fig. III - 4 CSAMT Interpreted Resistivity Sections (Section C and D in Fig. III-6)

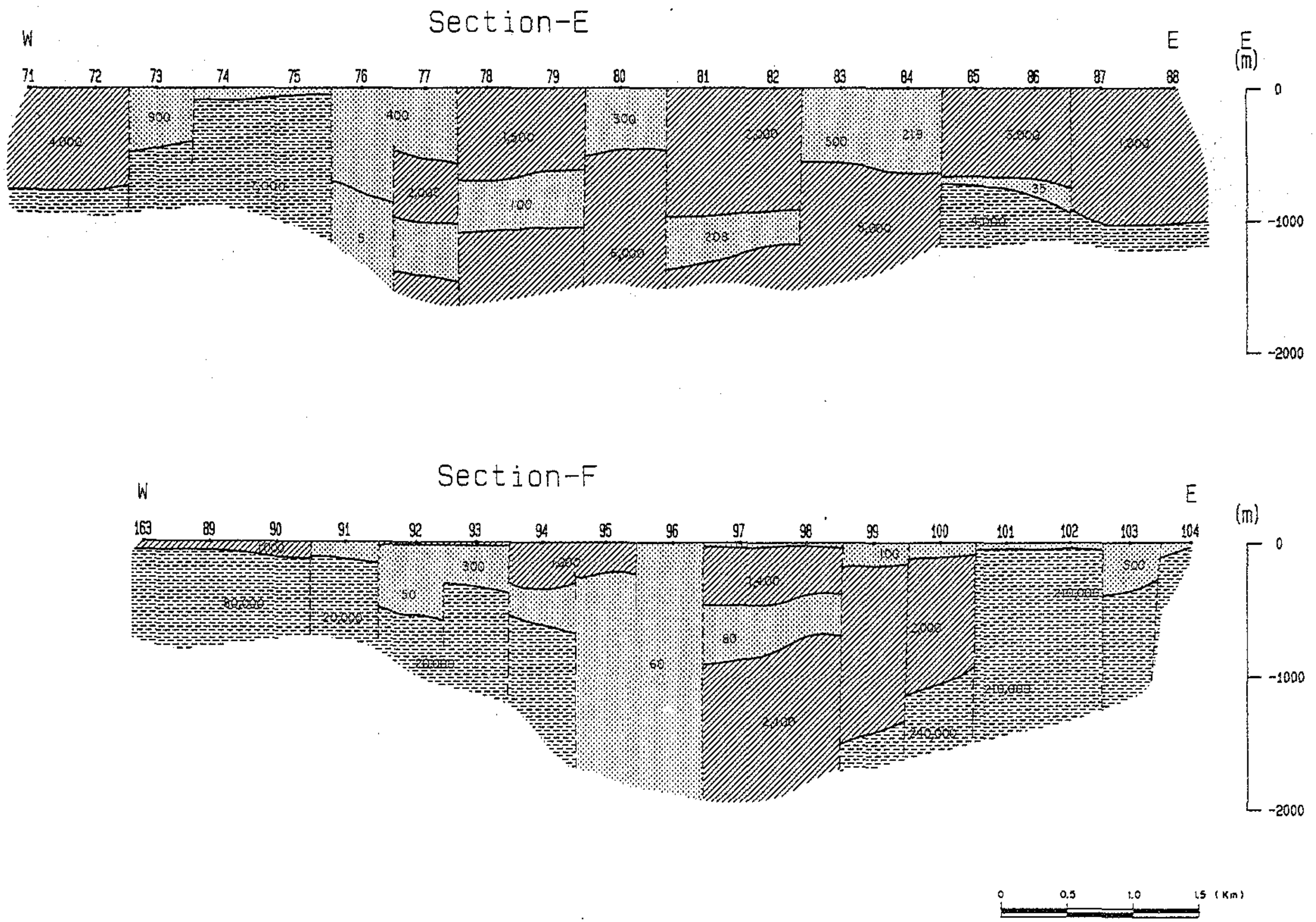

Fig. III - 5 CSAMT Interpreted Resistivity Sections (Section E and F in Fig. III-6)

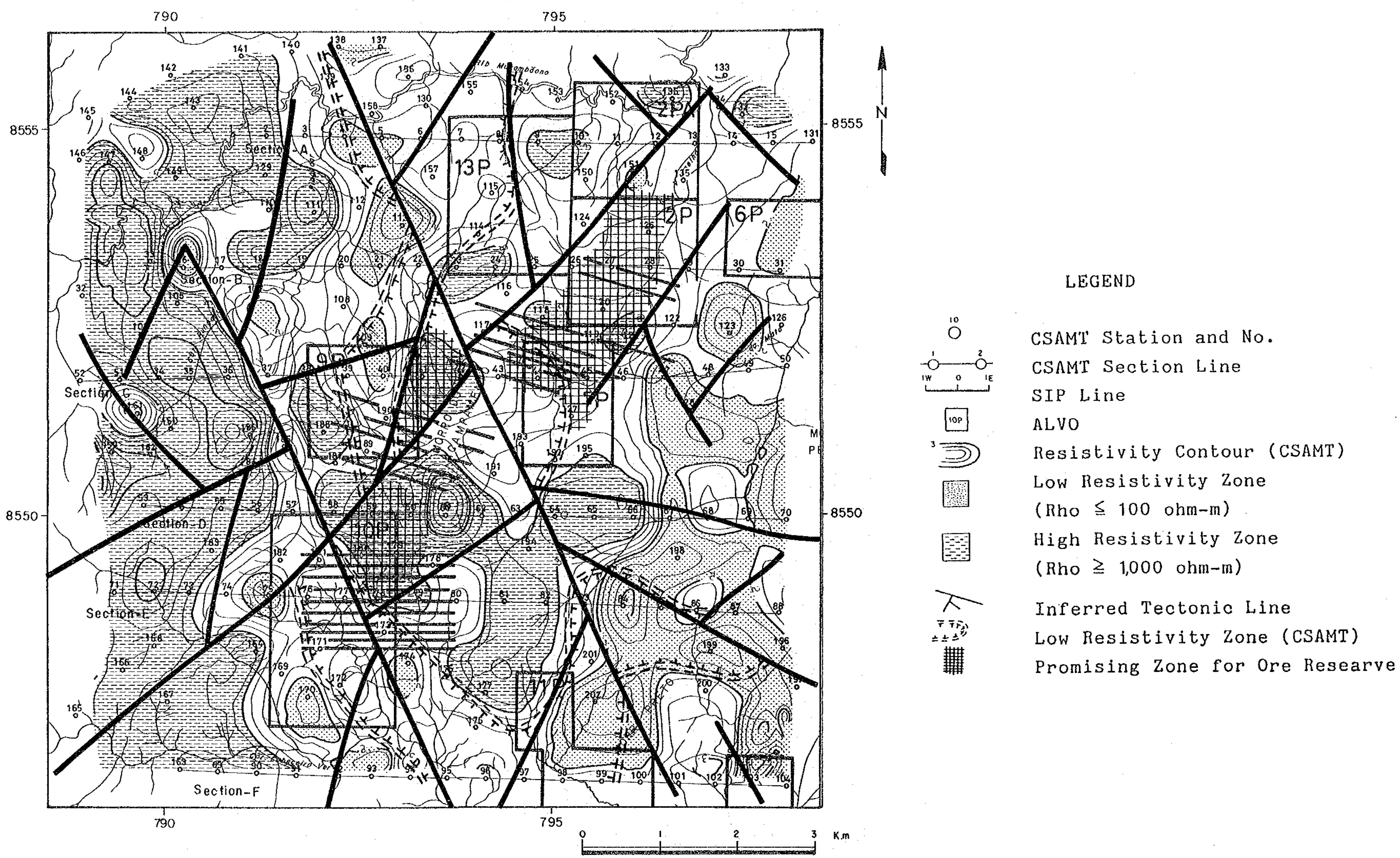

Fig. III - 6 CSAMT Interpretation Map (Morro do Acampamento Area)

The distirbution of resistivity in this area shows a concave structure in the central part.

Near the C-1 ore body the resistivity of the shallower zone (50m thick) is below 100Ω·m, and becomes more than 4,000Ω·m for the deeper zone. The C-1 ore body is hosted in upper zone.

In the plane map, the ore body is in the zone trending north east where the value of resistivity gradually changes.

Therefore, in the area with such a resistivity distribution possible mineralization similar to the C-1 ore body may be found.

4–2 SIP Method and IP Method

4–2–1 Contents of the Survey

Both SIP and IP methods measure IP phenomena induced by electric and ionic conductivity.

Two kinds of frequencies were used for the IP method. Frequencies ranging from 0.1 Hz to 100 Hz were also used for the SIP method to measure magnitude and phase differences. From those measurements the properties and shapes of anomalous sources to induce IP phenomena are discriminated. And spectral characteristics from rocks and/or ore deposits are discriminated from SIP method. Among sulfide minerals, graphite and others that being IP anomalies, pyrite and graphite generally induce stronger IP pheromena than chalcopyrite, galena and sphalerite.

Therefore, it is difficult, if not impossible to judge from the IP anomalous values alone whether a massive sulfide deposit of chalcopyrite, galena and sphalerite exist inside a larger pyrite dissemination. A composite interpretation is essential with using the differences of spectral patterns from the SIP method.

Contents and amount of the survey are shown in Table III–5. For both the SIP and IP methods the interval between electrodes is 100m and the factor is 1 to 5.

In Phase I, SIP lines trending east-northeast were set up just above and south of the C-1 ore bedy. In Phase II, SIP lines trending east-northeast were set up in the area including the southwestern IP anomalous area of Phase I and the geochemically anomalous zone around Morro do Acampamento.

In Phase III, ten IP and SIP lines trending east were set up side by side and another SIP line trending north was also set up in the area with geochemical anomalies in Alvo 10P, located southwest of Morro do Acampamento.

Table III - 5 Amounts of SIP and IP Survey

Phase	Survey Method	Line Name	Line Length	Points
I	SIP	Line-15S	1,300m	39
	SIP	Line-35S	1,300m	39
	SIP	Line-110S	1,300m	39
	SIP	Line-150S	1,400m	44
II	SIP	Line-110S	1,500m	46
	SIP	Line-130S	1,500m	48
	SIP	Line-150S	1,500m	49
	SIP	Line-160S	1,500m	28
	SIP	Line-170S	1,500m	49
	SIP	Line-190S	1,500m	49
	SIP	Line-270S	2,100m	79
	SIP	Line-290S	1,500m	49
	SIP	Line-310S	1,800m	64
	SIP	Line-330S	1,500m	49
	SIP	Line-350S	1,500m	49
III	SIP	Line-1345S	2,000m	74
	SIP	Line-1375S	2,000m	74
	SIP	Line-1405S	2,000m	74
	SIP	Line-1420S	1,800m	64
	SIP	Line-1430S	2,000m	74
	SIP	Line-1450S	2,000m	74
	SIP	Line-20E	1,600m	54
	IP	Line-1330S	2,000m	80
	IP	Line-1360S	2,000m	80
	IP	Line-1390S	2,000m	80
	IP	Line-1420S	2,000m	80
	IP	Line-1440S	2,000m	80

* Total 27Lines (IP Survey : 5Lines, SIP Survey : 22Lines)
* Total 1,490Points (IP Survey : 400 points, SIP Survey : 1,208 points)

4–2–2 Results of the Survey

(1) Area including C-1 ore deposit

In the area including the C-1 ore deposit, low resistivity area with less than 300Ω · m extends in a north south direction between higher resistivity areas with more than 300Ω · m. The C-1 ore body occurs above a depth of 50m. The resistivity is around 300Ω·m in the depth between 100 and 150m and more than 1000Ω·m in the deeper part. The former value lithologically correlates to schists (Pip_4 vxt_1), the latter correlates to amphibolites (Pip_3).

IP anomalies are observed in the resistivity zone with more than 300Ω·m. Strong IP phenomena are detected in higher resistivity zones. The shape of the IP anomalous zone is assumed to be induced by an anomalous source with either network and/or disseminated minerals. The known massive ore deposit, C-1, is shallow and possibly grades into network and/or disseminated ore in the deeper amphibotite units. So, it was thought that the network and/or disseminated sulfide minerals cause a IP anomary at central parts of Line 15S and 35S.

Characteristics of spectra from shallow massive sulfide deposits and from deep disseminated mineralization were discerned. Shown in Cole-Cole diagram, the latter (Figure III–8(B)) increases the value of imaginary part at high frequency range greater than the former (Figure III–8(A)).

(2) Morro do Acampamento Area

The area is sub-divided into two blocks, called block north and block south. The distance between them is 800m. In block north an IP anomaly was detected and in block south a geochemical anomaly was located during Phase I (Fig. III–7).

Apparent resistivities in this survey area show a clear distribution pattern; the high resistivity zone of more than 1,000 Ω·m at the Morro do Acampamento, and the apparent resistivity zone of less than 1,000 Ω·m at its surrounding area. At the boundaries between both zones there can be seen strong resistivity contrasts which suggest the existence of geological boundaries and/or fault structures. As iso-apparent resistivity lines in the north-south direction are preminantly distributed, a resistivity structure with a northern trend are dominant in this survey area.

(Block North)

IP indications are found in the area of the $Pip_4 vxt_1$ layer, and show a spectral pattern (Figure III–8(C)) attributes to small amounts of sulfide minerals. These sulfide minerals seem to be the dissemination type in the whole area, judging from the distribution pattern of IP indication appears to reflect the concentration of sulfide minerals. By means of two dimensional model analysis for these IP indications, two IP anomalous sources, are inferred in places shallower than 70m and in the places deeper than 150m.

A shallower anomalous source is located in a high resistivity zone in the vicinity of 150S line and vanish near 160S line. A Deeper anomalous source extends to the south with a slight inclination and dips to the east. It does not exist in the north of the 150S line.

(Block South)

Apparent resistivities are clearly classified into three zones, high, medium and low. High and medium zones are found at the Morro do Acampamento and at the western foot of the Morro do Accampamento, respectively, the low zone is distributed at the western part of the block. These zones are arranged in a north-south direction, so it is of clear that apparent resistivity distribution reflects the geological structure with northern trends in the area.

Two IP indications were disstributed in this block; one is found in the distribution area of the $Pip_4 vxt_2$ layer found at the Morro do Acampamento, and another one in the apparent resistivity zone of 100 Ω·m to 300 Ω·m at the western ends of the Lines 270S, 310S 330S and 350S. The former (Fig. III–8(D)) show a spectral pattern attributed to sulfide dissemination, and the latter (Fig. III–8(E)) show peculiar spectral pattern, which were not detected in the C-1 ore body, with a strong IP effect due to graphite-quartz schist and sulfide minerals.

It has been thought that if a graphite-quartz schist is distributed at gentle west-dipping angle like the distribution of the low resistivity layer of less than 100Ω-m, sulfide minerals would exist stratiformly in amphibolite below graphite-quartz schist. However, the deep spectral pattern was distinctly affected by graphite-quartz schist. A Graphite-quartz schist mixed with sulfide minerals were disclosed by drilling at depth.

(3) Alvo 10P Area

In this area, the high apperent resistivity zone is distributed in a wide area, while a low apparent resistivity zone is distributed in the south.

The low apparent resistivity zone extends to a depth of 150m from the surface and changes into a high apparent resistivity at depth. Though the schist distributed in this area has lower resistivity values than that of amphibolite, a low apparent resistivity zone is possibly affected by surface weathering and the presence of water and/or by a brecciated zone or clay zone. A low apperent resistivity zone caused by a possible fractured zone is situated inside the high resistivity area. This tendency is stronger in the deeper part. The low apparent resistivity zone extend northeast and northwest. The zone trending northeast is assumed to incline to the east. On the other hand, the high resistivity zone has a rectangular shape made by some faults and correlates to the area of schist. The resistivity changes in the area of high apparent resistivity is probably caused by intercalation of quartzite, amphibolite and amphibole schist beds with different resistivity in Pip_4.

IP anomalies are mainly distributed in following three area. These anomalies are thought to be caused by the same kind of source (Fig. III–7).

(1) Southern part

(2) Southeastern part

(3) Northern part

IP anomaly of (1) is distributed inside low to medium apparent resistivity zone which is thought to be caused by a fractured zone based upon the shape in pseudo-section. The shape is thought to be formed by an anomalous source of disseminated mineralization distributed near the surface.

IP anomaly of (2) is obtained in the middle to high apparent resistivity zone with a slight change of resistivity values. Anomalous areas of (1) and (2) are possibly caused by the same source, nevertheless they have different spectra shown in Figure III–8(F) and (G). The spectral pattern of anomary (1) attributes to pyrite. Though the spectral pattern from anomaly (2) resembles that from pyrite, it seems the possibility of existing another sulfides. According to two dimentional simulation of the shape of the anomaly (2), the source is proposed to have are approximate elliptic shape.

IP anomaly of (3) is gained inside the area of high resistivity and is thought to be composed of three sources based upon the pseudo-section. Based upon the plane distribution of IP and geochemical anomalies of Cu, Pb and Zn, possible mineralization is thought to exist in the area. The part with the strongest IP anomaly is interpreted to be the center of mineralization based upon model simulation.

Spectral patterns from the massive ore body discovered with drilling PM-138-GO done by CRRM is not very different from the one derived from IP anomalies around the drilling site, therefore it is very hard to delineate massive sulfide deposits inside a pyrite dissemination.

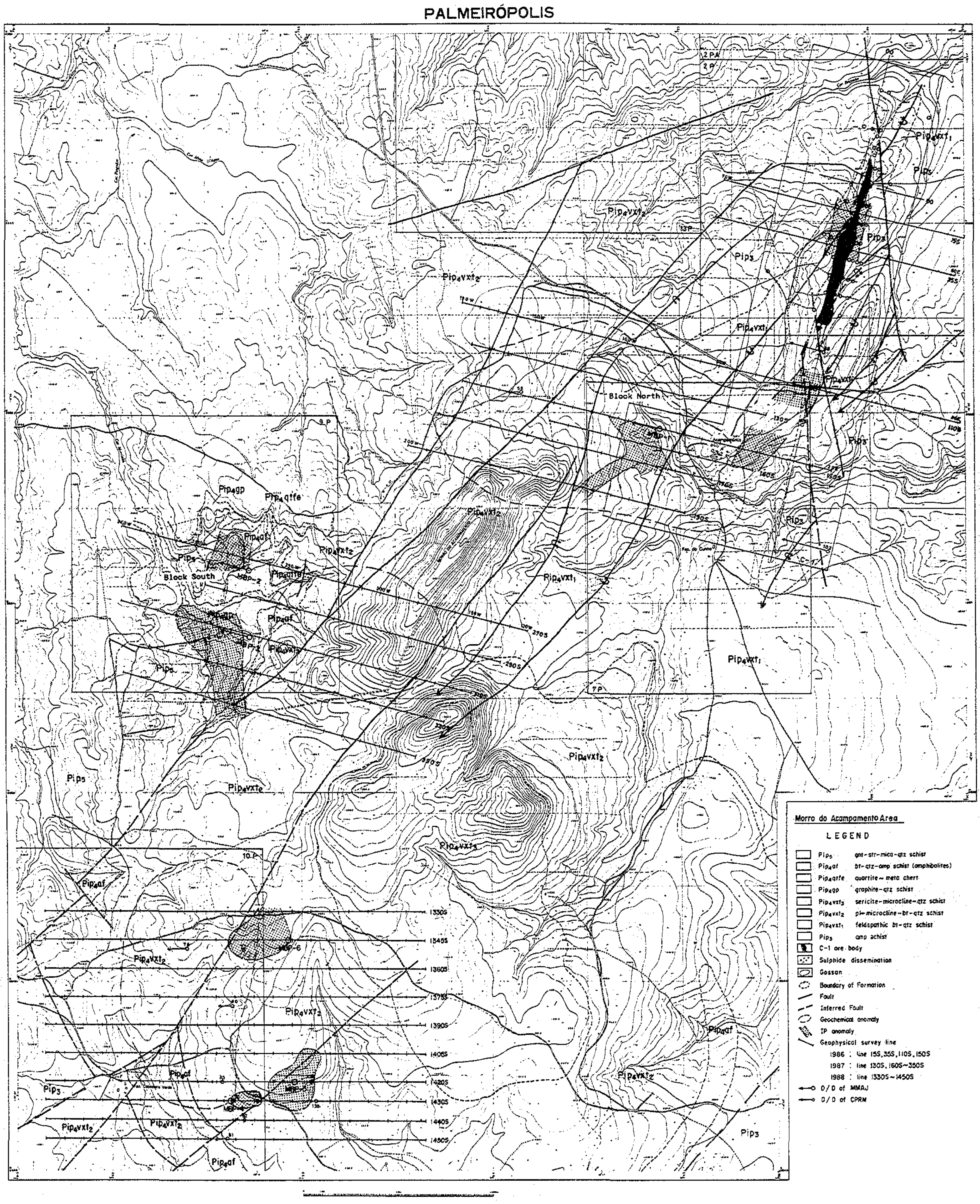

Fig. III-7 SIP·IP Interpretation Map in Morro do Acampamento Area

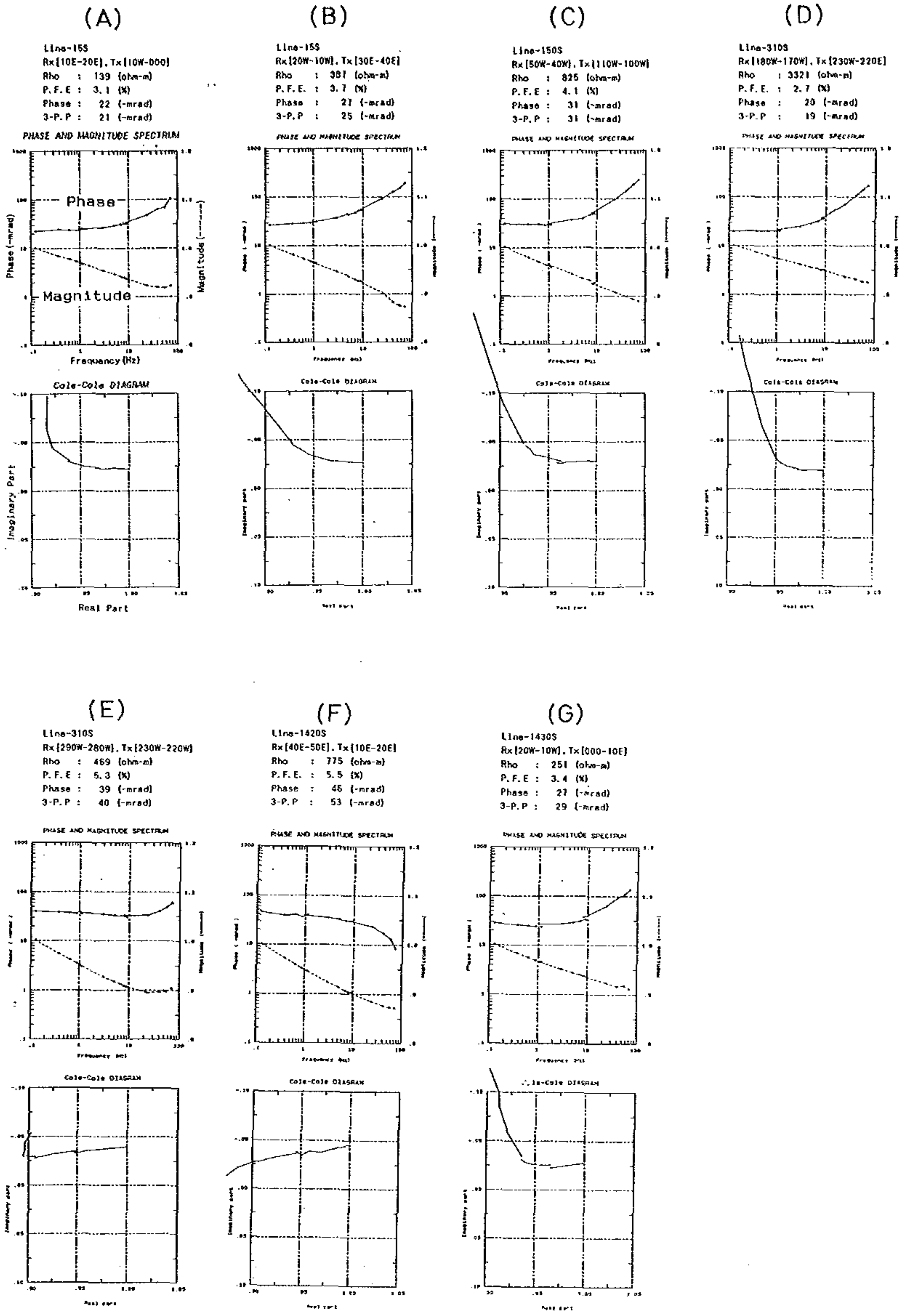

Fig. III-8 Typical SIP Spectra obtained in the Morro do Acampamento Area

CHAPTER 5 DRILLING

5–1 Contents of the Survey

In the west-southwest of Morro do Acampamento, in the center of the Morro do Acampamento area, 3 holes (900.37m) were drilled with the purpose to clarify the characteristics of the geophysical anomaly discovered using the SIP method in Phase II. 3 holes (1201.77m) were also drilled in Phase III with the purpose to clarify the geochemical anomaly, to pursue laterally known mineralization, to find different mineralized horizons and to clarify the characteristics of geophysical anomalies determined by SIP and IP methods in the Alvo 10P area. The total length of 6 holes was 2102.14m.

Drilling was carried out using conventional methods by GEOSOL. The diameter of the holes at the bottom was NX size. Core recovery was over 99.9% for each hole.

The location of each hole is shown in Fig. III–7. The outline of the drilling survey is described in Table III–6.

5–2 Result of the Survey

Geology and mineralization of each hole are as follows :

1. MBP-1 (depth: 300.15m, azimuth:285°, inclination: -60°)

The purpose of this hole was to elucidate the source of the IP anomaly detected by geophysical survey (SIP method).

The geology is mainly composed of garnet-muscovite-biotite-quartz schist, inter calated with beds of amphibolite-chlorite-biotite-schist in the upper part. All the beds are correlated to $Pip_4 vxt_1$.

Pyrite dissemination, which was assumed from the IP anomaly, was not found. The sections where pyrite was present, were assayed. The results of the chemical assay for sections of core with pyrite are as follows. Cu, Pb and Zn contents are all very low.

Depth (m)	Au (ppm)	Ag (ppm)	Cu (ppm)	Pb (ppm)	Zn (ppm)	S (%)
34.50 – 35.00	–	Tr	6	77	121	0.002
87.00 – 87.50	–	Tr	24	15	86	0.05
113.50 – 114.00	–	Tr	130	33	218	0.24
193.50 – 194.00	–	Tr	58	53	159	0.12
266.50 – 267.00	–	Tr	4	19	60	0.001

2. MBP-2 (depth: 300.12m azimuth: 285°, inclination: -60°)

The purpose of this hole was to elucidate the source of the IP anomaly detected below a depth of 150m by geophysical survey (SIP method).

The geology is composed of amphibobite and graphite-quartz schist of Pip_4 down to 168.20m from the surface and garnet-staurolite-muscovite-biotite-quartz schist of Pip_5 from 168.20m to 300.12m . Beds were thought to be inverted by folding according to the evidence of stratigraphy.

Disseminations of pyrrhotite, pyrite and chalcopyrite were observed at the upper most horizen of Pip_4. The disseminations were correlated with the source of the IP anomely. The result of the chemical assay for these sections of cores with sulfide minerals are shown below. Zn shows maximum value of 1.0 wt% (of 1m of core) at the uppermost horizon of Pip_4. Other elements have low values. Mineralizations were not strong.

Depth (m)	Au (ppm)	Ag (ppm)	Cu (ppm)	Pb (ppm)	Zn (ppm)	S (%)
29.00 – 29.50	–	Tr	71	6	114	0.54
62.50 – 63.00	–	Tr	68	9	67	0.13
94.50 – 95.00	Tr	Tr	106	8	182	0.37
114.50 – 115.00	Tr	Tr	71	6	108	1.37
150.00 – 151.00	Tr	Tr	71	9	117	1.67
151.00 – 152.00	Tr	Tr	94	6	141	2.49
152.00 – 153.00	Tr	Tr	141	11	244	2.60
165.00 – 166.00	Tr	Tr	101	9	1014	0.97
166.00 – 167.00	Tr	Tr	63	9	234	0.51
167.00 – 168.00	Tr	Tr	45	11	128	0.27
195.00 – 195.50	–	Tr	79	20	37	0.002

3. MBP-3 (depth: 300.10m, azimuth: 285°, inclination: -60°)

The purpose of this hole was to elucidate the source of the IP anomaly detected during geophysical survey (SIP method) below a depth of 150m.

The geology is composed of chlorite-biotite-quartz-amphibole schist with graphite-quartz schist from the surface down to 144.00m. Below this depth there are mainly of garnet-staurolite-muscovite-biotite-quartz schists intercalated with graphite-quartz schist of Pip_5.

Beds were also thought to be inverted by folding from the evidence of the stratigraphy of the core.

Disseminations of pyrrhotite and pyrite were observed in the chlorite-biotite-quartz-amphibole schist of the upper most horizon of Pip_4. Some disseminations of pyrite, pyrrhotite and chalcopyrite are also found in Pip_5. The dissemination zone is nearly correlated to the source of the IP anomaly.

A very small quantity of pyrite, chalcopyrite and pyrrhotite were observed as disseminations in Pip_5.

The result of chemical assay for these sections of cores are shown below. The values are all low. However the values in Pip_4 are higher than that of Pip_5 by one unit.

Depth (m)	Au (ppm)	Ag (ppm)	Cu (ppm)	Pb (ppm)	Zn (ppm)	S (%)
139.50 – 140.50	Tr	Tr	62	14	216	0.78
140.50 – 141.50	Tr	Tr	71	22	345	1.71
184.50 – 185.50	–	Tr	64	14	79	0.002
221.50 – 222.50	–	Tr	88	21	65	0.03

4. MBP-4 (depth: 400.00m, vertical)

The purpose of this hole was to pursue the lateral extension of the mineralization intersected with drilling (PM-52-GO) conducted by CPRM and to check whether some other mineralized horizons exist below the known mineralization.

Geology of this hole is mainly composed of muscovite-biotite-quartz schist, biotite-quartz schist and garnet-muscovite-biotite-quartz schist with intercalations of amphibole-biotite-schist beds from the surface down to 287.65m. The rock from 287.65m to 350.10m is amphibolite (Pip_4 af) with intercalations of biotite-quartz schist. From 350.10m down to 400.00m the rock mainly comprises garnet-muscovite-biotite-quartz schist with beds of amphibolite in it. The geological structure of this area is thought to show homoclinal structure dipping northeast.

Disseminations of pyrite with small veinlets of minor sphalerite galena and chalcopyrite were observed in the muscovite-biotite-quartz schist in the section shallower than 80m. The dissemination is thought to continuous from that of PM-52-GO. Small scale banded and massive pyrrhotite mineralization was observed between garnet-muscovite-biotite-quartz schist and amphibolite in the depth range 286.6m to 287.65m. Slightly disseminated pyrrhotite is also observed in the amphibolite below the banded and massive pyrrhotite.

The results of the chemical assay for these sections of core are as follows. The values are higher than those of MBP-1, MBP-2 and MBP-3. That shows stronger mineralization.

Depth (m)	Au (ppm)	Ag (ppm)	Cu (ppm)	Pb (ppm)	Zn (ppm)	S (%)
28.50 – 29.25	<0.05	<2	150	470	572	2.0
29.25 – 30.05	<0.05	3	142	1486	0.54*	2.2
30.05 – 31.05	<0.05	10	248	668	1928	1.8
43.40 – 44.20	<0.05	8	1608	3700	1.2*	2.7
44.20 – 44.80	0.05	9	212	3872	1.1*	2.3
44.80 – 45.25	<0.05	<2	34	152	160	1.6
65.10 – 66.10	<0.05	4	142	1592	3960	1.0
66.10 – 66.60	<0.05	18	267	4294	0.69*	1.7
66.60 – 67.35	<0.05	<2	37	120	184	0.60
67.35 – 67.80	<0.05	<2	56	492	1078	0.86
67.80 – 68.65	<0.05	<2	42	228	550	0.84
68.65 – 69.55	<0.05	<2	88	380	784	1.2
69.55 – 70.45	0.10	<2	47	170	272	1.5
70.45 – 71.35	<0.05	7	92	3320	4140	1.9
71.35 – 72.40	<0.05	6	117	2470	4800	2.2
72.40 – 73.65	<0.05	3	86	986	2480	1.1
73.65 – 74.65	<0.05	<2	48	40	106	0.22
77.95 – 78.35	<0.05	2	192	492	1116	0.68
286.60 – 286.85	<0.05	<2	98	25	12	3.0
286.85 – 287.20	<0.05	<2	42	30	32	1.0
287.20 – 287.65	<0.05	<2	550	46	39	7.2

* : %

5. MBP-5 (depth: 400.45m, vertical)

The purpose of this hole was to elucidate the source of the IP anomaly detected at depths of 100m to 200m during the geophysical survey (IP method).

Rocks are mainly composed of staurolite-garnet-muscovite-biotite-quartz schist, muscovite-biotite-quartz schist and biotite-quartz schist with intercalation of amphibolite beds. All of these were correlated to Pip_4.

Small scale drag folds whose enveloping surface extend sub-parallel to the direction of the long axis of the core were frequent that large scale folds were thought to exist in this area. The axis of these folds was inferred to trend northeast with the axial surface of the fold dipping to the southeast from the surface geology.

Pyrite dissemination with small amount of sphalerite, galena and chalcopyrite were observed in muscovite-biotite-quartz schist in the central part of this hole. This dissemination nearly corresponds to the source of the IP anomaly.

The result of the chemical assay for this section of core is shown below. From the point of view of the mineralization MBP-5 is thought to be continuous to MBP-4. The mineralization of MBP-5 is weaker than MBP-4.

Depth (m)	Au (ppm)	Ag (ppm)	Cu (ppm)	Pb (ppm)	Zn (ppm)	S (%)
61.50 – 62.00	<0.05	<2	52	274	1934	0.74
205.00 – 206.00	<0.05	<2	232	28	1511	0.35
206.00 – 207.00	<0.05	<2	126	31	348	0.25
207.00 – 208.00	<0.05	<2	118	20	320	0.12
208.00 – 209.00	<0.05	<2	176	22	1239	0.27
209.00 – 210.00	<0.05	<2	130	20	604	0.17
210.00 – 211.00	<0.05	<2	184	17	748	0.17
211.00 – 212.00	<0.05	2	120	33	626	0.47
212.00 – 213.00	<0.05	<2	57	37	544	0.12
213.00 – 214.00	<0.05	<2	78	47	374	0.27
214.00 – 215.00	<0.05	<2	35	90	320	0.65
215.00 – 216.00	<0.05	<2	41	32	234	0.65
216.00 – 217.00	<0.05	<2	60	102	328	0.49
217.00 – 217.95	<0.05	<2	30	63	194	0.53
218.00 – 219.00	<0.05	<2	27	42	230	0.34
219.00 – 220.00	<0.05	<2	126	9	662	0.54
220.00 – 221.00	<0.05	<2	218	27	350	0.64
221.00 – 222.00	<0.05	<2	409	60	1012	0.57
222.00 – 223.00	<0.05	11	200	444	3540	0.42
223.00 – 224.00	<0.05	2	47	284	960	0.80
224.00 – 225.00	0.05	<2	57	290	1406	1.1
225.00 – 225.90	<0.05	<2	32	69	100	0.37

6. MBP-6 (depth: 401.32m, vertical)

The purpose of this hole was to elucidate the source of the IP anomaly found at depths above 150m by the geophysical survey (SIP method).

The rocks are composed of garnet-muscovite-biotite-quartz schist with some intercalations of biotite-quartz schist, biotite-amphibole schist and amphibolite and all rocks are correlated to Pip_4.

Small scale drag folds whose enveloping surface extend sub-parallel to the direction of long axis of core are so continuous in the middle section of the hole that large scale folds were thought to exist in this area. The trend of the fold axis and the inclination of the axial surface of the fold are thought to be the same as described above.

The dissemination zone composed mainly of pyrite were detected at 72–74 m, 216–224 m and below 369 m, contrary to geophysical expectation. The slight disseminations of pyrite with dots of very small amounts of sphalerite were observed near the bottom of the hole below 369 m. The values below 369 m is higher than those of other sections. The values are in general lower than those of MBP–4 and MBP–5. That shows lower mineralization.

Depth (m)	Au (ppm)	Ag (ppm)	Cu (ppm)	Pb (ppm)	Zn (ppm)	S (%)
72.00 – 72.95	<0.05	<2	16	13	83	0.52
73.00 – 74.00	<0.05	<2	17	18	84	0.82
216.00 – 217.00	<0.05	<2	14	11	56	0.24
217.00 – 218.00	<0.05	<2	11	7	65	0.11
218.00 – 218.95	<0.05	<2	14	9	60	0.11
220.00 – 221.00	<0.05	<2	9	10	80	0.10
221.00 – 222.00	<0.05	<2	13	12	58	0.25
222.00 – 223.00	<0.05	<2	14	8	68	0.24
223.00 – 224.00	<0.05	<2	16	6	52	0.25
369.50 – 370.50	<0.05	<2	104	14	948	0.36
370.50 – 371.50	<0.05	<2	34	15	228	0.41
371.50 – 372.50	<0.05	<2	218	17	228	0.11
387.50 – 388.50	<0.05	<2	25	11	134	0.31
388.50 – 389.50	<0.05	<2	21	9	262	0.31
389.50 – 390.50	<0.05	<2	20	8	232	0.28
394.00 – 395.00	<0.05	<2	14	9	182	0.10
395.00 – 396.00	<0.05	<2	25	10	356	0.087

The result of the chemical assay for these sections of core is as follows.

The above represents the outline of the geology and mineralization determined from drilling holes conducted over two years. The results from the drilling survey are summalized as follows:

(1) Three mineralized horizons were observed in the south and southwest of Morro do Acampamento area (Fig. III–9). The lowest horizon, partly composed of massive pyrrhotite, occurs between lower amphibolite (Pip_4 af) and the upper so-called mica schist (Pip_4). It was observed in drill hole MBP-4. Lithofacies of footwall and hangingwall are similar to the ones of the C-1 ore deposit (Ⓘⅱⅰ in Fig. III–9).

The middle horizon dissemination, composed of pyrite dissemination with very small veinlet of sphalerite, galena and chalcopyrite, occurs in the so-called mica schist in the middle horizon of Pip_4. It was interested by three holes, MBP-4, MBP-5, MBP-6. A massive ore body is thought to occur near the center of the mineralization, which was found with drilling (PM-138-GO) conducted by CPRM (Ⅱ in Fig. III–9).

The upper horizon, composed of slight disseminations of pyrite, pyrrhotite and chalcopyrite in graphite-quartz schist, occurs in the uppermost horizon of Pip_4. It was interested by drill holes MBP-2, MBP-3 (Ⅰ in Fig. III–9).

(2) The geologic structure of this area, folds whose axes trend northeast to north northeast, faults with similar strikes and other faults trending northwest, make this area very complicated.

Therefore it is very difficult to pursue the mineralized zone even if it is in one horizon.

Table III - 6 Summary of the Results of Drilling Survey

Year	No. of Holes	Purpose (Target)	Drilling Period	Azimuth	Inclination	Length (m)	Core Length (m)	Core Recovery (%)	Mineralization
Phase II 1987	MBP-1	An anomalous source detected by geophysical survey	Oct. 6 ~ Oct. 31	285°	−60°	300.15	299.91	99.9	almost no mineralization
	MBP-2	An anomalous source detected by geophysical survey	Oct. 23 ~ Nov. 20	285°	−60°	300.12	299.96	99.9	very weak dissemination of pyrite
	MBP-3	An anomalous source detected by geophysical survey	Nov. 5 ~ Nov. 26	285°	−60°	300.10	298.20	99.3	very weak dissemination of pyrite
Phase III 1988	MBP-4	Lateral extention of known mineralization & new mineralized horizon	Jun. 7 ~ July 1	–	−90°	400.00	399.65	99.9	weak dissemination of pyrite, sphalerite, galena, chalcopyrite in mica schist (Zn $\leqq$ 1.2%, Pb $\leqq$ 4294 ppm, Cu $\leqq$ 1608 ppm), massive and banded pyrhotite (286.70 m ~ 287.65 m deep) between mica schist & amphibolite
	MBP-5	An anomalous source detected by geophysical survey	Aug. 9 ~ Aug. 24	–	−90°	400.45	400.45	100	very weak dissemination of pyrite, sphalerite, galena, chalcopyrite in mica schist (Zn $\leqq$ 3540 ppm, Pb $\leqq$ 444 ppm, Cu $\leqq$ 409 ppm)
	MBP-6	An anomalous source detected by geophysical & geo-chemical survey	Aug. 25 ~ Sept. 7	–	−90°	401.32	401.32	100	very weak dissemination of pyrite, sphalerite, galena, chalcopyrite in mica schist (Zn $\leqq$ 948 ppm, Pb $\leqq$ 17 ppm, Cu $\leqq$ 218 ppm)

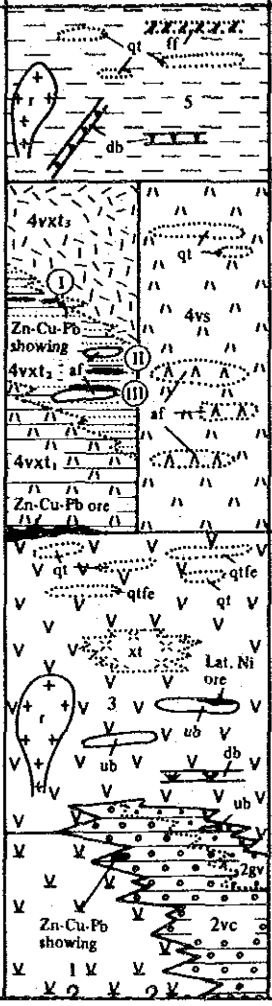

Geological Unit		Columnar Section	Lithology	Metallogeny
Palmeirópolis Volcano-Sedimentary Sequence (RIBEIRO FILHO and TEIXEIRA, 1981)	Pip		r : Filo granite 5 : str-bt-mv-qtz sch., ky-bt-mv-qtz sch., gnt-mv-qtz sch. and ky-str-mv-qtz sch. associated with basic sill and dyke (db), banded iron formation (ff) and quartzite (qt)	Fe in iron formation. Kyanite associated with quartzite along fault.
			4vxt₃ sc-mc-qtz sch. (rhyolitic composition) 4vxt₂ : pl-mc-bt-qtz sch. and pl-bt-qtz sch. intercalated with amphibolite (af) (rhyolitic to rhyodacitic composition) 4vxt₁ : feldspathic bt-qtz sch., str-gnt-bt-qtz sch., bt-anf sch., biotitite and cl. rock (dacitic to rhyodacitic composition) 4vs : feldspathic gnt-bt-qtz sch. and mica sch. including ky. and acidic meta tuff, with quartzite (qt) and amphibolite (af)	"Stratabound"-type volcanogenic Zn-Cu-Pb massive and disseminated sulfide ore deposits. (Corpo C-1 and Albo 10P) (I),(II),(III) were detected in "Palmeiropolis Project"
			3 : dark fine-grained amphibolite with quartzite (qt), ferruginous quartzite (qtfe), gnt-bt-mv-qtz sch. (xt) and basic to ultra-basic dyke (db, ub) r : Morro Solto granite 2gv : metagraywacke, metaconglomerate and ultrabasic sill (ub) 2vc : acidic to intermediate tuff, lapilli tuff, volcanic breccia and their schist 1 : gabbroic banded coarse-grained amphibolite	Volcanogenic Zn-Cu-Pb massive sulfide mineralization detected by drilling hole of Billiton Metais. Supergene lateritized Ni ore deposit concentrated with ultra-basic "sill" in mine claim of Billiton Metais.

Fig. III-9 Mineralized Horizon in Pip_4

PART IV RIO DOIS DE JUNHO AREA

CHAPTER 1 GEOLOGY

1–1 General Geology

Rio Dois de Junho Area, occuping the area of 150km^2, is located nearly at the center of the Palmeiropolis (whole) area.

Geological mapping was carried out concurrently with the geochemical soil sampling using a drainage map on a scale of 1:10,000 enlarged from a map with a scale of 1:50,000 and aerialphotos at a scale of 1:25,000. The geology was compiled on a geologic map at a scale of 20,000.

Regional geology of the surrounding area of the Rio Dois de Junho area consists, from the base upward, of the Archaean Cana Brava basic-ultrabasic massif (Acb) which occurs in the east of this area and composes the basement rock of the Project area, lower Proterozoic Palmeiropolis volcano-sedimentary Sequence (Pip), middle Proterozoic Serra da Mesa group (Pmsm, Pm) which occurs in the far west, Rio Maranhão cataclastic zone (ct), and upper Proterozoic Paranoa Group (Pspa).

Palmeiropolis volcano-sedimentary sequence, which occurrs as a zone, is classified into five into five members, Pip_1, Pip_2, Pip_3, Pip_4, and Pip_5 (DNPM/CPRM, 1983), and shows an arrangement trending NE-SW∿N-S.

Small intrusives also occur.

1–2 Detailed Geology

Palmeiropolis volcano-sedimentry sequence (Pip_1∿Pip_5) is solely found in this area. One third of the western part of the area is occupied by Pip_5. In two-thirds of this area, younger formations are distributed from both east and west toward the center. Strikes of formations are generally northeast in the northern half of the area and north in the southern half of the area.

1–2–1 Stratigraphy

(1) Pip_1 Member

Distribution:

The member is the lower most geology in the area and distributed at the end of northeastern part on a small area.

Lithofacies:

The rocks is dark green, consisting of gabbroic coarse-grained amphibolite. The exposure of the fresh rock is limited to the areas along the rivers. The weathering parts become reddish brown fine-grained soil.

(2) Pip_2 vc Member

Distribution:

The member is distributed on a very small scale in the northeastern and eastern limits.

Lithofacies:

The rocks are gray to brown lateritized schist containing muscovite, biotite, feldspar and quartz. Grains of garnet were recognized in the eastern limits.

Granitic rocks are found in parts of the northeastern limits where the floating stones consist of pegmatite locally.

(3) Pip_3 Member

Distribution:

The member shows a form of two zonal arrangements from northeastern to eastern part and from north to southwestern part.

Lithofacies:

The rocks consist mainly of dark greenish gray fine-grained compact amphibole schist. There is a banded texture consisting of leucocratic part with quartz – plagioclase and containing melanocratic part of amphibole, and/or lenticular quartz near the Pip_4 vx member locally. The member is intercalated with quartzite (qt), ferruginous quartzite (qtfe) and mica-quartz schist (xt).

(4) Pip_4 vs Member

Distribution:

The member is widely distributed from the northeastern to the southern parts occupying about half of the area.

Lithofacies:

The rocks consist of gray feldspar-muscovite-biotite-quartz schist to gneiss in fresh part, and reddish brown mica-quartz schist in weathering part.

The member is intercalated with quartzite (qt) and amphibolite (af). The latter shows the same lithology as the Pip_3 member and consists mainly of dark greenish gray fine-grained amphibole schist.

(5) Pip_5 Member

Distribution:

The member is distributed from the north to the southwestern parts and widely occurs outside of the area.

Lithofacies:

The rocks are composed of yellowish to reddish brown colored garnet–mica–quartz schist. Staurolite fragments of one centimeter in maximum length are observed in places 500m west from the boundaries with the Pip_3 member in the northwestern parts. The member is locally intercalated with quartzite (qt) and light gray compact calc-silicate rocks (cs). The member is intruded by basic sills and dykes (db).

1–2–2 Intrusives

The intrusive rocks in the area are composed of granitic rocks (γ) and basic rocks (db).

(1) Granitic Rocks (γ)

Distribution:

The rock is distributed in the central northern part trending in a NNE–SSW direction and having about 1.2km length with about 200m width.

Lighology:

The rock is light gray and granoblastic muscovite–granite consisting of crystals of two millimeters in average diameter and is accompanied by muscovite–K-feldspar–quartz pegmatite containing crystals more than five millimeters locally. The rock includes some xenoliths of gneissose rocks which are similar to the fresh rocks of the Pip_4 vs member. The boundaries between granitic and gneissose rocks are unclear either in their field occurrences or under microscopic observation.

Time of intrusion:

It is thought that the granite intruded in early to middle Proterozoic (JICA/MMAJ, 1986).

(2) **Basic Rocks (db)**

Distribution:

the rocks occur slightly in the Pip_5 member.

Lithology:

The rocks consist mainly of green to dark green colored coarse-grained amphibolite and locally contain fine-grained gabbro. The rocks are partly accompanied by sulphide – quartz veinlet and sulphide dissemination.

1–2–3 Structure

According to the distribution of rocks, strike and bedding of thin layers intercalated, characteristics of soil and photogeology, geologic structure of NE–SW system in distinct. Namely, the successions between Pip_3 and Pip_4 vs members are symmetrically distributed on the synclinal axis (partly overturned) at slightly east of the central part.

Fault systems of NE–SW and NW–SE directions are distinct. Compared with the sense of dislocation of horizontal component of both fault structures, the NE–SW system is right-lateral fault and the NW–SE system is left-lateral fault; therefore, these systems are considered to form a conjugate set.

The dominant direction of schistosity is almost parallel to the distribution of the members.

CHAPTER 2 MINERALIZATION

Two mineral showings, such as gossans on the boundary between Pip_4 vs and Pip_3 members in the eastern end and sulphide dissemination in the basic intrusive rocks of the northern part, are observed.

Some floats of gossans, having one meter in maximum diameter, consist of limonite with quartz networked veinlets and are scattered on an area of 50 meters in diameter. The assay result shows trace of Au ·Ag, 0.00% of Cu ·Pb and 0.01% Zn.

The sulphide minerals are recognized as dissemination and in quartz network veinlets in the basic intrusive rock. According to the microscopic observation, granular pyrrhotite dots the gangue minerals and shows the paragenesis with a small amount of chalcopyrite, magnetite and pentrandite. No small amount of Ti–minerals are also observed.

CHAPTER 3 GEOCHEMICAL SURVEY (SOIL)

3–1 Contents of the Survey

Soil geochemical surveys were done in the Rio Dois de Junho area where Cu-Pb-Zn geochemical anomalies have been obtained by the Phase I stream sediment survey and Pip_4 formation corresponding to the ore bearing horizon is distributed.

The purpose of the surveys of Phase II were to clarify the distribution of the Pip_4 formation and do the best to find any mineralized showings by the geological survey, and to delineate the anomalies in detail by the geochemical soil survey.

Sampling was done using a drainage map at 1:10,000 enlarged from the 1:50,000 scale map, and air photographs at 1:25,000.

Concurrently, two thousand and eight soil samples were collected at the average sampling density of 13 to 14 samples per square kilometer. The sampling was carried out along the main roads and rivers. In addition, offset survey lines were set by clearing in order to make distribution of sampling stations as even as possible over the whole area.

The samples collected were chemically analyzed by the atomic absorption method for the following three target components: Cu, Pb and Zn. The data were statistically processed using single component analysis and multivariate analysis methods.

(1) Single Component Analysis

Histograms and cumulative frequency distribution diagrams were made in order to extract anomalous values of each component (Figure IV–1).

Determination of anomalous threshold value was made based on the method used by Sinclair (1974). Owing to the inflection point in each cumulative frequency distribution diagram, Cu and Zn are divided into three populations: anomalous population (hereinafter referred to as A polulation) and two background populations (hereinafter referred to as B(I) and B(II) populations). Pb was divided into two populations: A population and background population B. The threshold values of each element were determined by comparing one percent value with 99% value of each population (Table IV–1).

Table IV–2 shows correlation matrix of each component, in which Cu and Zn show a strong positive correlation.

(2) Multivariate Analysis

Two factors were extracted by factor analysis in the same manner as in the first phase (Table IV–3). The first factor is Zn-Cu, and thc second Pb-Cu(-Zn).

3–2 Results of the Survey

(1) Single Component Analysis

The anomalous values of each component obtained in the data processing stage were plotted on the drainage map (Figure IV–2).

In Phase I, the analysis was performed by lithofacies because content levels of each component in Morro do Acampanento area were different in respective lithofacies (basic and schistose rocks). In this area, only the analysis of the entire samples was done because the contents levels were found more or less the same.

Copper (Cu)

The areas occupied by Group III (from 41 ppm up to below 56 ppm), including one percent of A population, 24% of B(II) population and 0.9% of B(I) population, are almost consistent with those of amphibolite. Group II (56 ppm or more and lower than 95 ppm), consisting of 73%of A population and 17% of B(II) population, is recognized in areas of high copper content in the areas distributed by amphibolite. With regard to Group I (95 ppm or more), which is composed of 26% of A population and one percent of B(II) population, five concentrated zones are extracted in the areas of amphibolite and another five in other areas.

Lead (Pb)

The areas underlain by Groups I and II are not consistent with the distribution of lithofacies. Group I (35 ppm or more) includes 80% of A population and 1% of B population, and Group II, 22 ppm or more and less than 35 ppm, includes 19% of A population and 27% of B population. As to the zones occupied by Group I, however, those in schistose rocks region rather than amphibolite region are extracted. Two concentrated zones were found in the Pip_4 vs member in slightly south of the central part.

Zinc (Zn)

Geochemical anomalous zones of Zn exhibit the same distribution as that of Cu anomalous zones. Namely, the areas of distribution of both Groups II and III almost correspond to those of amphibolite. Group II, 37 ppm or more and less than 70 ppm, includes 45% of A population, 90.5% of B(II) population and one percent of B(I) population. Group III, from 31 ppm up to below 37 ppm, consists of one percent of A population, includes 7.5% of B(II) population and two percent of B(I) population. The areas of Group I (70 ppm or more) which is composed of 54% of A population and one percent of B(II) population, are also included in the areas of amphibolite. But except in the areas of amphibolite, four areas of Group I were extracted.

(2) Multivariate Analysis

Figure IV–2 (below) shows the analytical diagram of the first and second factors.

First Factor (Zn-Cu)

Based on the definitions that those with factor score of not less than 1.0 are the high factor score and those from 0.5 or more to less than 1.0 the moderate factor score, the zones of moderate to high factor scores were almost consistent with the areas underlain by amphibolite in the same way as the Cu and Zn anomalous zones extracted by the single component analysis.

The first factor is considered to reflect the characteristic of the country rock represented by amphibolite.

Second Factor (Pb-Cu-(Zn))

As the result of the analysis conducted in the same procedure as in the first factor, high factor score zones with those of 1.0 or more almost correspond to the area occupied by Group I of Pb.

The factor might be related with the lead mineralization.

The high scores of not less than 1.0 of the second factor supposed to be related to a type of mineralization are not concentrated much and have no remarkable trend, although they are observed more in the southwest than in the northeast.

Two small areas were delineated in an area underlain by the Pip_4 vs formation in the southern part, for the reason that the areas are overlapped by high anomalies for Cu, Pb and Zn and high scores of the second factor. One of the two, in the southern part, was thought to be promising because it was on the Pip_3. But it was very small.

However, there is few possibility of the same type of mineralization as that of the Palmeiropolis ore deposit, in the Rio Dois de Junho area, because the high score distributions of the second factor might be parallel with the amphibolite distributions, if the second factor is related with the same type of mineralization as the Palmeiropolis ore deposit supposed to be syngenetic and no remarkable mineralization is recognized.

Table IV - 1 Results of Simplified Statistical Treatment of Geochemical Data of Soil (Rio Dois de Junho Area)

	Values in ppm	Total data		Anomalous		Background (Ⅱ)		Background (Ⅰ)	
		%	No.	%	No.	%	No.	%	No.
Cu	Group Ⅰ ≧ 95	1.7	35	26	26	1	9	-	-
	Group Ⅱ ≧ 56	11.4	228	73	73	17	154	0.1	1
	Group Ⅲ ≧ 41	11.3	227	1	1	24	217	0.9	9
	Group Ⅳ < 41	75.6	1,518	-	-	58	524	99.0	994
	Max 196 / Min 3 / Mean 25.1	100	2,008	100	100 (5%)	100	904 (45%)	100	1,004 (50%)
Pb	Group Ⅰ ≧ 35	4.9	99	80	80			1	19
	Group Ⅱ ≧ 22	26.6	534	19	19			27	515
	Group Ⅲ < 22	68.5	1,375	1	1			72	1,374
	Max 200 / Min 4 / Mean 18.6	100	2,008	100	100 (5%)			100	1,908 (95%)
Zn	Group Ⅰ ≧ 70	8.7	174	54	163	1.0	11	-	-
	Group Ⅱ ≧ 37	56.8	1,141	45	136	90.5	999	1	6
	Group Ⅲ ≧ 31	4.9	98	1	3	7.5	83	2	12
	Group Ⅳ < 31	29.6	595	-	-	1.0	11	97	584
	Max 202 / Min 5 / Mean 23.0	100	2,008	100	302 (15%)	100	1,104 (55%)	100	602 (30%)

Table IV - 2 Correlation Matrix of three Elements of Geochemical Data of Soil (Rio Dois de Junho Area)

	Cu	Pb	Zn
Cu	1.000		
Pb	0.350	1.000	
Zn	0.713	0.211	1.000

Table IV - 3 Results of Factor Analysis of Geochemical Data of Soil (Rio Dois de Junho Area)

Factor Loadings (varimax rotation)			Communality
	Factor 1	Factor 2	
Cu	0.720	0.462	0.7315
Pb	0.098	0.587	0.3539
Zn	0.819	0.234	0.7255
Factor contributions	87.671%	14.291%	

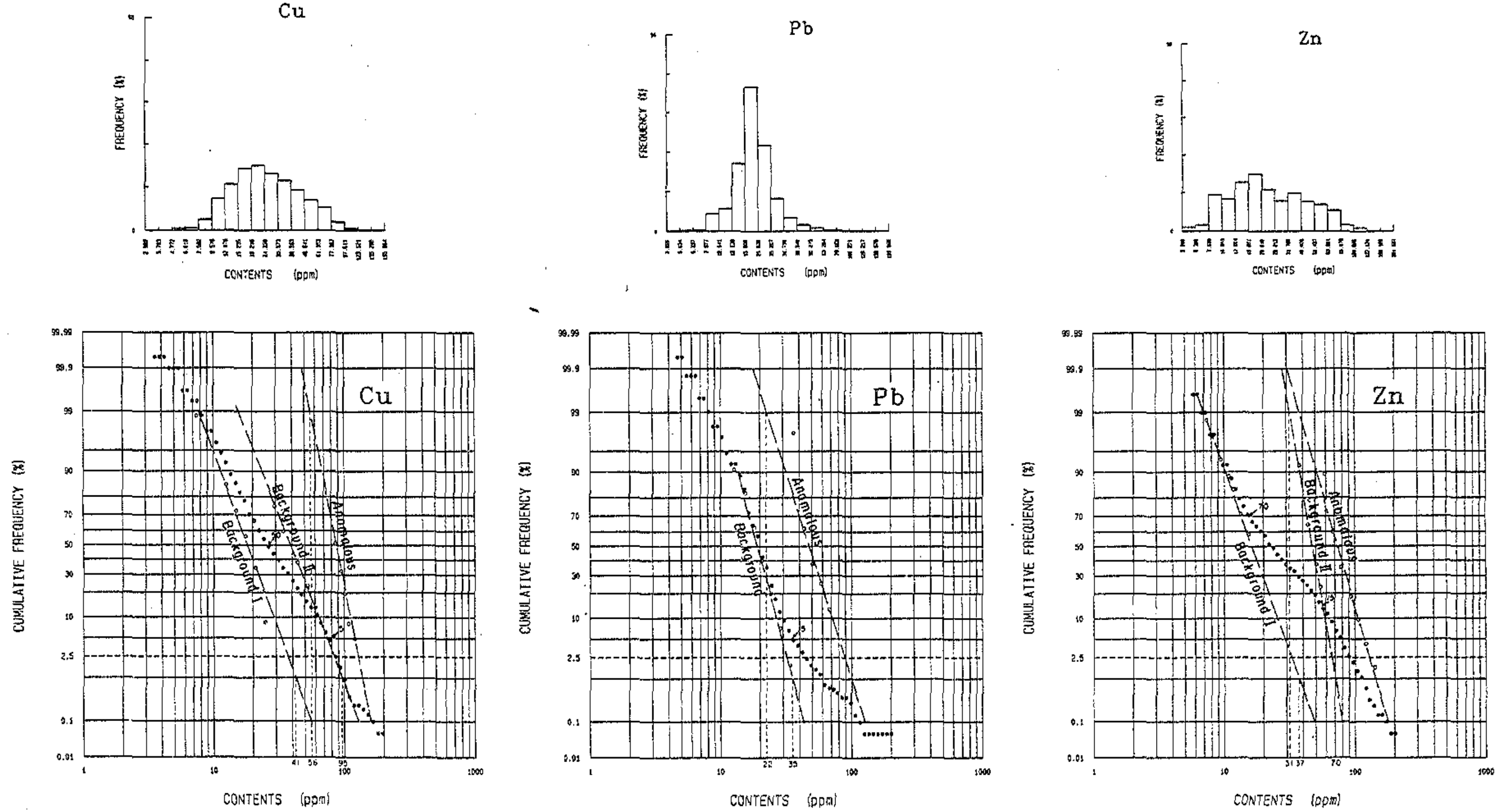

Fig. IV - 1 Histogram and Cumulative Frequency Distribution of Cu, Pb and Zn of Soil (Rio Dois de Junho Area)

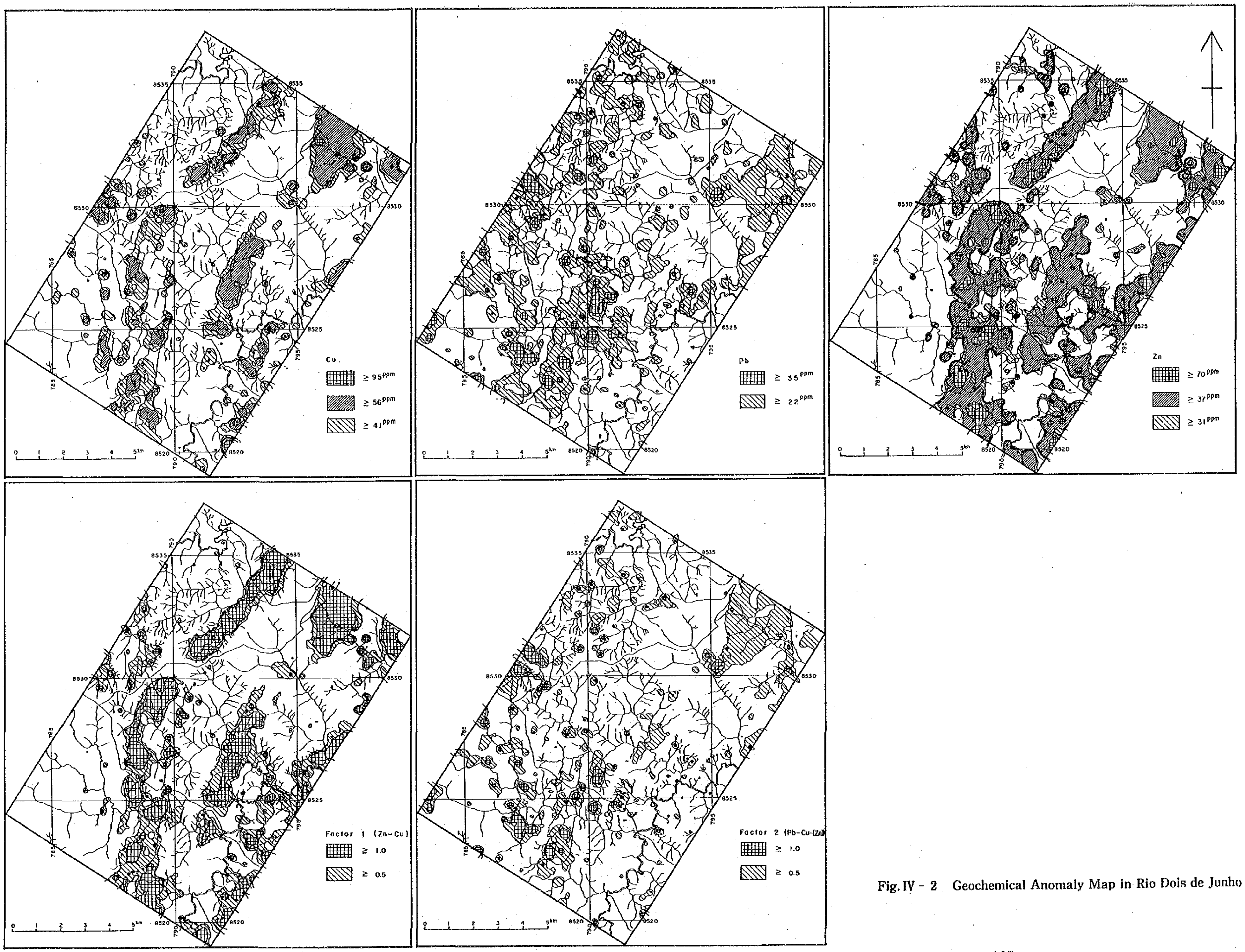

Fig. IV - 2 Geochemical Anomaly Map in Rio Dois de Junho Area

PART V CONCLUSIONS AND RECOMENDATIONS

CHAPTER 1 MORRO DO ACAMPAMENTO AREA

1–1 Conclusion

(1) As the result of geochemical survey using stream sediments, anomalous areas of Cu-Pb-Zn are found on Alvo 1P, 2P, 7P, 9P, 10P and 11P. As the result of soil geochemical survey, anomalous areas of Pb-Zn are found in Alvo 7P, 9P, 10P, 13P, and anomalous area of Cu is found in Alvo 11P. These anomalies are thought to be due to mineralization (Fig. II–7, Fig. III–2).

(2) The drilling executed on the area with IP and geochemical anomalies in Alvo 7P to the northeast of Morro do Acampamento could not delineate the possible mineralization. The target horizon was Pip_4 where Palmeiropolis ore deposits were located (Fig. III–7).

(3) The two drillings carried out on two strong IP anomalous areas in Alvo 9P to the southwest of Morro do Acampamento, confirmed dissemination of sulfide minerals (pyrite and pyrrhotire) in a section spaced 70m to 100m from the core. The maximum amount of sulfide minerals is about 7 wt%. Thin beds of graphite-quartz schist were also found in the same area (Fig. III–7).

(4) The three drillings carried out on three IP anomalous areas to the east of Alvo 10P located in the southwest of Morro do Acampamento, yielded pyrite dissemination with small amounts of chalcopyrite, galena and sphalerite (Fig. III–7).

(5) The disseminated zones are thought to be related to each other because they are present next to each other or very close; the host rocks are all mica schist; sulfide minerals in the host rocks and their occurrences are similar to each other; and geophysical techniques disclosed a continuity in the zones. The Cu-Pb-Zn massive sulfide deposit was simultaneously detected in one of the IP anomalous areas by drilling carried out by CPRM. The massive sulfide deposit was concluded to be continuous into the pyrite dissemination zones.

(6) From the above mentioned, the Morro do Acampamento area, especially the south of Morro do Acampamento, should be finaly evaluated by further detailed survey which will permit the determination of the scales and the reserves of the ore deposits.

(7) IP and SIP methods were effective for the detection of the pyrite dissemination. However, they were not able to discriminate Cu-Pb-Zn sulfide minerals in the pyrite dissemination zones neither to localize the Cu-Pb-Zn ore deposit in the dissemination zones. That was thought to be due to the fact that the scale of Cu-Pb-Zn massive sulfide deposit (determined by PM-138-GO) was too small to the pyrite dissemination zone and that the Cu-Pb-Zn sulfide minerals dispersed in the dissemination zones (determined by MBP-4, MBP-5, MBP-6, etc.) were too little compared to the amount of pyrite. IP and SIP methods seemed to have shown a limitation in the determination of the presence and localization of Cu-Pb-Zn sulfide minerals included in a pyrite dissemination on a wide scale.

1–2 Recomendation

(1) As clarified by Phase II and Phase III of the survey, the stratified Cu-Pb-Zn deposits are present at least at the bottom, middle and top of Pip_4. Geophysical (SIP, IP methods) and drilling surveys are recommended for further exploration in the area of Pip_4, where geochemical anomalies are left unsurveyed.

(2) Carry out detailed geophysical and drilling survey in the areas of southwest of Morro do Acampamento where the IP anomaly zones need of a more detailed study.

(3) A more detailed survey using geophysical and drilling methods is recommended to evaluate the ore reserves, especially to the east, northeast and southwest of the known mineralized area. Since the massive ore deposit was found in the mineralized area in the east of Alvo 10P.

(4) Carry out rock geochemistry to reveal the stratigraphy of the ore hosting field using drilling cores in the Morro do Acampamento area. Carry out inclined drillings directing northwest and arranged in northeast direction, since in this area the shape of the ore deposits are thought to be controlled by the folds with NE trending axis and SE dipping fold axial planes.

CHAPTER 2 RIO DOIS DE JUNHO AREA

2–1 Conclusion

In the area, geochemical surveys by stream sediments were conducted in Phase I, and a detailed geochemical survey using soil sampling were carried out in Phase II. As the result of the above surveys, geochemical anomalies of Cu, Pb and Zn were found in Pip_4. However, as compared to the size of the Palmeiropolis deposit, the anomalous zones found in these areas are so small that in case of the existence of an ore deposit, it would be rather uneconomically small.

2–2 Recomendation

Further surveys are not recommended. Because even if ore deposits were found, it would be uneconomical in this area.

REFERENCES

(1) Almeida F.F.M., Hasui Y., Brito Neves B.B. and Fuck R.A. – 1981 – Brasilian structural provinces; an introduction, Earth-Sci., Rev., 17: 1-29.

(2) Almeida F.F.M. e Hasui, Y. – 1984 – O Precambriano do Brasil.

(3) CNEN/DNPM/CPRM – 1973 – Levantamento Aerocintilometrico Projecto Serra da Mesa.

(4) CNEN/DNPM/CPRM – 1977 – Projeto Serra da Mesa II-Goias, Relatorio Final.

(5) CPRM – 1984 – Projeto Plameiropolis Informe Tecnico.

(6) DNPM – 1975 – Carta Geologica do Brasil ao Miliodesimo, Folha Goias SD-22.

(7) DNPM/MME – 1981 – Projeto RADAMBRASIL, Vol. 25.

(8) DNPM – 1981 – Geologia e Inventario dos Recursos Minerais do Regiao Central do Estado de Goias – Projeto Brasilia –.

(9) DNPM – 1981 – Os Principais Depositos Minerais do Regäo Centro-Oeste.

(10) DNPM – 1983 – Levantamento Aerogíofisico do Projeto Palmeiropolis-GO.

(12) DNPM – 1983 – Garimpos do Brasil.

(13) DNPM – 1984 – Garimpos do Brasil.

(14) DNPM – 1984 – Geologia do Brasil

(15) DNPM – Projeto Mapas Metalogeneticos e de Previsão de Recurais Minerais – Porangatu – Folha SD-22-X-D.

(16) DNPM – Projeto Mapas Metalogeneticos e de Previsão de Recurais Minerais – Alvorada – Folha SD-22-X-B.

(17) Whitten, E.H. Timothy – 1966 – Stractural Geology of Folded Rocks, Rand Mc. Nally & Company.

(18) Girardi A.V. and Kurat G. – 1982 – Precambrian Mafic and Ultramafic Rock of the CANA BRAVA Complex, Brasil.

(19) Hasui Y. et al. – 1980 – Datacoes Rb-Sr e K-Ar Centro Norte do Brasil e seu Significado Geologico-Geotectonico, XXXI Congresso Brasileiro de Geologia.

(20) Guilbert, John M. and Park, Charles F. Jr. – 1986 – The Geology of Ore Deposits, W.H. Freeman and Company

(21) Louis L. – 1978 – Aspectos Geotectonicos da Africa Ocidental a Leste do Golfo da Guine com Refrencia as Conexoes Estruturais e Litoloficas Brasil e Africa, XXX Congresso Brasileiro de Geologia.

(22) Meyers, R.E. and MecLean, W.H. – 1983 – The geology of the New Inco copper deposit, Noranda district, Quebec, CAN. J. EARTH SCI., Vol. 20, 1291-1304.

(23) Miyashiro, A., – 1965 – Metamorphic Rocks and Metamorphic Belt, Iwanami Shoten (in Japanese)

(24) MMAJ – 1979 – Report on Technical Development for Mineral Exploration-SIP Method (in Japanese)

(25) MMAJ – 1985 – Report on Morro Agudo and Palmeiropolis Project, Brasil.

(26) JICA/MMAJ – 1986, 1987 – Report on the Cooperative Mineral Exploration in the Palmeiropolis Area, Federative Republic of Brazil.

(27) Sato, Takeo. – 1983 – Kuroko-type Deposits in Earth's History, The Society of Mining Geologists of Japan, Mining Geology Special Issue No. 11. (in Japanese)

(28) Severin, P.W.A. – 1982 – Geology of the Sturgeon Lake Copper-Zinc-Lead-Silver-Gold Deposit, CIM. Bull., Vol. 75, 107-123.

(29) Sinclair, A.J. – 1974 – Selection of Threshold Values in Geochemical Data Using Probability Graphs, J. Geochem. Explo., 3, 129-149.

(30) Suszczynski, E. – 1981 – South America, Structural Framework, Chapter 13 in Precambrian of the Southern Hemisphere. ed by D.R. Hunter, ELSEVIER

CPRM: Companhia de Pesquisa de Recursos Minerais

DNPM: Departamento Nacional da Produção Mineral

MMAJ: Metal Mining Agency of Japan

JICA: Japan International Cooperation Agency